

Coexistence of Hardening and Softening Phenomena in Elastomeric Polymers under Nano-Impact Loading

Amritesh Kumar and George Youssef*

This article reports the coexistence of hardening and softening phenomena when polyurea is submitted to repeated nano-impacts with various impact forces while controlling the strain rate. The manifestation of these phenomena is further elucidated by interrogating ultraviolet irradiated samples under ambient and nitrogen atmospheres, wherein artificial weathering accelerates hardening by reducing the nano-impact depths as a function of exposure duration while increasing the impact load, nano-impact repetitions and strain rate sensitivity favored softening. A 21% and 48% increase in indentation depth are recorded after 100 repetitions at a relatively higher force (10 mN) at a low strain rate and low force (2.5 mN) at a relatively higher rate for pristine and weathered polyurea, respectively. Electron microscopy evidences the induced, progressive damage at the nanoscale based on the agglomeration of hard segments, reduced free volume, and weathering-induced surface embrittlement.

1. Introduction

Pursuing optimal protective armor for civilian, policing, and military applications continues to attract assiduous research seeking impact-resilient and shock-tolerant materials. With emphasis on bulk polymeric materials, aromatic polyurea has recently emerged as a candidate with benignity to a broad range of environmental, loading, and operating conditions at different strain rates.^[1-6] The remarkable performance of polyurea has been associated with the nano-segmented microstructure consisting of hard and soft domains augmented with ubiquitous hydrogen bonding, improving strength and stiffness.^[7,8] However, nanoscale mechanical behavior in dynamic loading scenarios remains ambiguous despite some efforts in the microscale.^[9]

A. Kumar, G. Youssef
Experimental Mechanics Laboratory, Department of Mechanical
Engineering
San Diego State University
5500 Campanile Drive, San Diego, CA 92182, USA
E-mail: gyoussef@sdsu.edu

The ORCID identification number(s) for the author(s) of this article can be found under https://doi.org/10.1002/mame.202400134

© 2024 The Author(s). Macromolecular Materials and Engineering published by Wiley-VCH GmbH. This is an open access article under the terms of the Creative Commons Attribution License, which permits use, distribution and reproduction in any medium, provided the original work is properly cited.

DOI: 10.1002/mame.202400134

The compliant nature of aromatic polyurea stemming from the soft domains and the mechanical resiliency based on the interspersed hard domains gives rise to multiscale mechanical behavior.[7,8] The high entropic cost of this thermoset elastomer is also conducive to forming hydrogen bonding between the amino and carbonyl groups within the nearby urea motifs within the macromolecular structure.[10-12] However, several other dissipation mechanisms have been proposed using hybrid experimental and computational investigations of the polyurea macromolecule to decipher the remarkable mechanical properties.^[6] The mechanisms encompass multiscale phenomena, including the Vogel-Fulcher-Tammann process, reversible pseudo-plasticization, deformation localization at domain boundaries,

soft segment mobility, and shear-resistance coupling with ballistic compressive loading. [13-20] The strain rate is at the essence of these competing mechanisms, activating concurrent processes to effectively dissipate the incoming mechanical energy irrespective of the loading rate. [5,6,21,22] Vitrification was observed at a low strain rate and high compressive stresses due to pressure-driven glass transition. [6,23] At the same time, increased segment affiliation resulted in enhanced material stiffness under hydrostatic compression due to the contraction of the mean spacing of the interchain hydrogen-bonded hard segments.^[20] Aromatic polyurea showed plastic deformation and signs of adiabatic shearing when submitted to ultrahigh strain rate loading, which was also associated with conformational changes.[22,24] In addition to the aforementioned experimental studies, deep learning analysis-based determination of dynamic, cohesive properties of polyurea beyond the dynamic fracture toughness has been studied in.^[25] Therefore, the hierarchical molecular structure and nanoscale strengthening contrivances cooperate to improve the dynamic toughness of polyurea. Nonetheless, while imperative for fundamental and holistic understanding, the nanoscale impact behavior of aromatic polyurea must be vigorously explored to probe and reveal the processes responsible for single and multiple impact scenarios, i.e., the primary motivation leading to this article.

Herein, the nanoscale mechanics of aromatic polyurea are revealed using novel nano-impact experiments on a nanoin-dentation instrument, elucidating the coexistence of hardening and softening phenomena as a function of loading conditions (standoff distance, applied load, and number of impacts). Benefiting from surface embrittlement due to controlled artificial



www.mame-journal.de

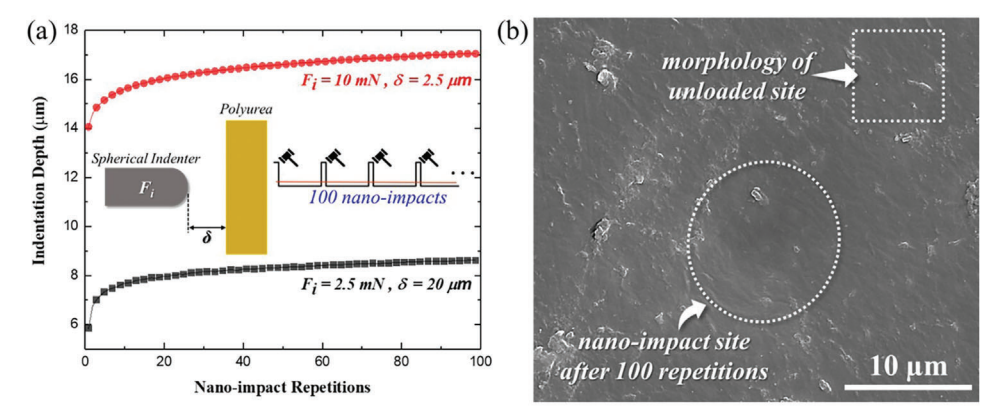


Figure 1. a) Indentation depth as a function of the number of nano-impacts of aromatic polyurea at two loading conditions. b) SEM image delineating the morphological differences between unloaded and impacted sites ($F_i = 10 \text{ mN}$ and $\delta = 2.5 \text{ }\mu\text{m}$).

weathering, e.g., ultraviolet radiation, a pronounced hardening phenomenon is reported while exaggerating the cumulative damage nearly absent from unexposed polyurea samples. The novelty of the research leading to this report stems from (1) the exploitation of nanoindentation framework to induce nanoimpacts at different loading conditions and (2) the leverage of the weathering effect to amplify the coexistence of hardening and softening phenomena.

2. Results and Discussion

Figure 1a shows the maximum indentation depth resulting from repeated nano-impacts (the measurements approach is schematically depicted in the inset) as a function of impact force and standoff distance, elucidating their corresponding effects. The impact sites were chosen after careful reconnaissance using a high magnification optical approach to avoid imperfections and voids to avoid biasing the nano-mechanics results by rough surface morphology. The results in Figure 1a indicate that a fourfold force increase corresponded to a twofold higher indentation depth compared to an eightfold change in the standoff distances, averaging over 100 successive nano-impacts. The dichotomy between the indentation depths indicates a higher sensitivity of polyurea to nano-impact forces than the strain rate (due to the increase in velocity from a longer standoff distance). Higher applied loads activate softening mechanisms via decreased segmental affiliation and chain sliding accommodations by the free volume. [26–28] The soft segment contributions dominate the response at a lower loading rate, giving rise to a compliant behavior, i.e., the reported softening phenomena. However, continuous nano-impact pounding over the same site translated to a 21% increase in indentation depth after 100 repetitions, demonstrating the incremental decrease in deformation resistance as a function of repeated impacts and highlighting the mechanism responsible for the impact-resiliency of aromatic polyurea, i.e., relative chain sliding supported by the complementary shear stresses. It is imperative to note that the discussion herein focuses on the collective evolution in the indentation depth, i.e., comparing the initial depth to the final one, which is consistent with the creep response (time-dependent behavior) of polyurea. The creep modulus was previously found to significantly reduce as a function of time under constant loading, e.g., our recent report. [21] Furthermore, the limited duration between the repeated nano-impacts (\approx 2 s) resulted in accumulated indentation depth since the loaded sites had insufficient time to relax fully.

On the other hand, at a relatively higher strain rate ($\varepsilon \approx 5 \text{ s}^{-1}$, which is ≈16× higher than the other loading condition discussed above), the stiffness of the hard segments is the primary influence of the mechanical response, exemplified by lower indentation depths. A higher loading rate (i.e., longer standoff distance) hardens polyurea by increasing segmental affiliation, resisting the indenter penetration to higher depths. However, the indentation depth increased by 48% as the polyurea sample endured 100 nano-impacts, activating an additional softening mechanism due to the viscoelastic properties of the macromolecule and clarifying the coexistence of softening and hardening phenomena as a function of loading conditions. Remarkably, nano-impacts from long standoff distances result in undetectable damage, while repeated impacts at 10 mN from shallower standoff distances transpired as faint permanent imprints only observable under the scanning electron microscope (SEM). Figure 1b shows the nanoimpacted sites (compared to a nearby pristine/unloaded area that was not impact loaded) under the latter conditions exhibiting permanent surface dimples, exemplifying minor evidence of plastic deformation. The recoverability of polyurea is associated with the underlying elasticity of the entangled chains in the crosslinked framework supported by the reversibility of the free volume. [22,29]

It is well-established that extended ultraviolet exposure degrades elastomeric polyurea through photoinduced chain scission, oxidation, and hydrogen bonding evolution mechanisms, [8.9,12.30,31] resulting in pronounced embrittlement and amplifying progressive damage in the nano-impact sites. Hence, ultraviolet-exposed polyurea samples were examined using the nano-impact experiment described above to exaggerate the cumulative damage as a function of pounding repetitions. Figure 2 summarizes the nano-impact results of ultraviolet-exposed polyurea as a function of the exposure duration (virgin to 15 weeks), radiation atmosphere (ambient and nitrogen), and nano-impact conditions (impact force, 2.5 and 10 mN, and stand-off distance, 20 and 2.5 μ m, respectively). The indentation depth is tightly coupled to these experimental variables. The depth initially increased exponentially as a function of the nano-impact



www.mame-journal.de

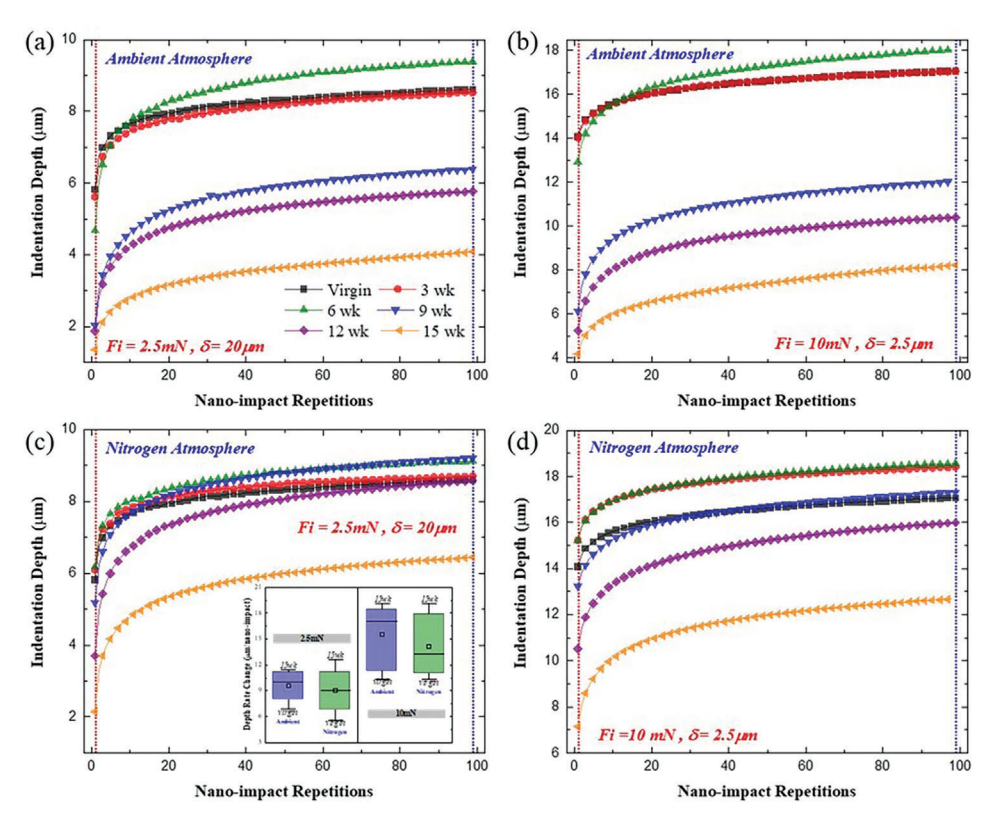


Figure 2. Evolution of nano-impact indentation depth after ultraviolet exposure in ambient (top panel) and nitrogen (bottom panel) atmospheres as a function of impact force and standoff standing.

repetition due to the availability of free volume, allowing compaction of the material under the indenter tip, compliance of the unloaded sites sinking the indenter deeper, and uninterrupted interspersion of the hard segments within the soft domain matrix. Soon after, i.e., within <20 nano-impacts, the indentation depth plateaus, irrespective of the exposure duration and atmosphere or the impact conditions because of the work hardening effects stemming from the transfer of repeated strain energy onto the impact sites and the slow recovery of the progressively damaged impacted continuum due to distinct viscoelastic properties of polyurea, e.g., creep behavior. The weathering-induced embrittlement is also associated with increased hard segment affiliation, transpiring as a notable reduction in the indentation depth as a function of exposure duration. Moreover, the rate of change in the nano-impact indentation depth (slope of each curve within the last 70 nano-impact is compiled in the inset in Figure 2c) as a function of repetition within the plateau region evolved as the exposure duration increased. While the depth rate change is ubiquitously higher in the 15 weeks samples than the virgin counterpart, irrespective of the radiation atmosphere and the nano-impact conditions, its deviation from the mean exemplifies a dependence on these experimental parameters. This evolution provides more evidence for the coexistence of the revealed hardening and softening phenomena, substantiating the prominence of elastomeric polyurea for impact mitigation applications.

The culmination of the nano-impact experiment on virgin and ultraviolet-exposed polyurea samples is presented in **Figure 3**,

evidencing the hardening phenomenon due to the weathering senescence mechanisms, as well as the softening due to the increase in applied load (Figure 3b), higher nano-impact repetitions, and strain rate sensitivity. The indentation depth decreased as a function of the exposure duration, irrespective of the radiation atmosphere and nano-impact conditions, exemplified by limited penetrations compared to virgin materials. In other words, the extended weathering activated stiffening processes such as surface embrittlement, hard segment agglomeration, and increased chain affiliations, which, in turn, severely limited the indentation depth as the exposure duration increased. This interrelationship between the exposure duration and reduction in indentation depth evidences the hardening phenomenon. It is then worth noting that the nitrogen atmosphere curbed the extent of the hardening mechanisms due to the preservation of the intermolecular hydrogen bonding affinities relative to the exposure under ambient conditions, as shown using several spectroscopic techniques a priori.[12] The suppression of the hardening mechanism under nitrogen atmosphere gives rise to the counter, but coexisting, softening phenomenon, such that the indentation depth for the samples radiated in ambient conditions was consistently inferior, irrespective of the duration, force, and strain rate. Nonetheless, increasing the nano-impact force coincided with a notable increase in indentation depth, irrespective of the strain rate, attributed to softening. The indentation depth in the virgin samples nearly doubled after 100 nano-impacts at 2.5 mN load and 20 µm standoff distance compared to only 21% when impacted with 10 mN at 2.5 µm.

- AcroOlecular

Materials and Engineering

www.mame-journal.de

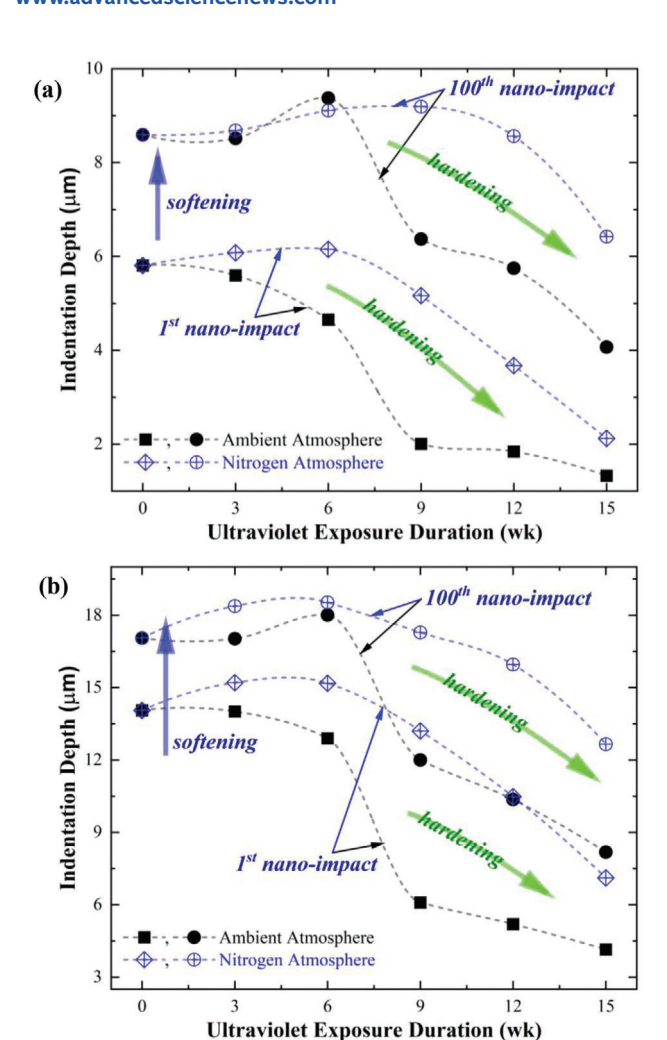


Figure 3. Manifestation of hardening and softening phenomena due to extended ultraviolet duration and repeated nano-impacts, respectively, as a function of nano-impact conditions a) 2.5 mN and 20 μ m, and b) 10 mN and 2.5 μ m.

The difference in nano-impact depths highlights the strain rate sensitivity of polyurea, where longer standoff distance translates to higher impact velocity (relatively higher strain rate). The inference about the strain rate sensitivity as a function of the nano-impact repetitions was consistent, irrespective of the sample condition (e.g., pristine or ultraviolet-exposed). The interdependence between the softening, e.g., higher indentation depth, the impact force, and the number of successive nano-impacts, also transpired, suggesting the contributions of the deformation mechanisms (stretching and sliding) of the soft segments as a function of all experimental variables.

The nano-impact craters, after 100 successive repetitions, elucidated the dichotomy stemming from the weathering atmosphere. Figure 4 comprises a collage of SEM micrographs collected from the surface of nano-impacted samples after 15 weeks of continuous ultraviolet exposure, differentiating the morphology of the surrounding surfaces and the crater imprints from pounding at 2.5 mN impact force. Figure 4a shows the five impact sites, exemplifying similar failure damage characterized by

a deep imprint surrounded by an uplifted rim from the evacuated material from the progressive damage caused by the indenter tip. On the contrary, Figure 4b depicts the impact crater from the same loading condition but of 15 weeks sample exposed under a nitrogen atmosphere, where the imprints are rimless with no sign of accumulated debris around the impact sites. The rimless craters in the latter indicate higher material compaction under the indenter, which is attributed to the preserved ductility of polyurea even after extended exposure duration. This coincides with the conclusions above about the source of the softening phenomenon and superficial protection of the nitrogen provided to the polyurea samples during the weathering process, i.e., limiting the aging mechanism to only photodegradation. On the other hand, the rimmed craters in the impacted ambient samples further support the ongoing hypothesis of ultraviolet-induced photooxidation, chain scission, and restructuring of the hydrogen bonding motifs within the macromolecule. The latter assertion is in excellent agreement with our previous thermogravimetric^[8] and spectroscopic^[12] about the contributions of hydrogen bonding, ubiquitous in this polyurea structure, to the overall response.

3. Conclusion

This article presents a comprehensive nanomechanics study of polyurea elastomer with segmented microstructure as a function of nanoscale impact measurements. The influence of impact force and strain rate (i.e., standoff indenter distances) was explored. A higher impact force at a lower strain rate resulted in higher penetration depths than a lower nano-impact force at a higher rate. Furthermore, nanoscale impact characterization was applied to ultraviolet-irradiated polyurea samples to exaggerate the uncovered phenomena due to weathering-induced surface degradation. After multiple nano-impacts, a 21% and 48% increase in indentation depth were recorded after 100 repetitions at high force at a low strain rate and low force at a higher rate, respectively, exemplifying unexpected softening behavior at higher strain rates. The nano-impact studies revealed the coexistence of hardening and softening phenomena, further exemplified in irradiated polyurea under ambient and nitrogen atmospheres. The hardening characteristics were attributed to evolution in segmental affiliation, agglomeration of hard segments, and reduced free volume. The softening behavior was associated with the stretching and sliding deformation mechanisms of the soft segments. SEM analysis of the impacted sites supported the coexistent hardening/softening phenomena in the elastomeric polyurea. Thus, this study not only unlocks a new methodology to study the mechanics of elastomers but also reports novel inferences that would aid in designing more efficient and reliable impact-resistant coatings by incorporating the effects of environmental weathering.

4. Experimental Section

Aromatic polyurea thin sheets were prepared by step polymerization upon mixing oligomeric diamine (Evonik) and modified diphenylmethane diisocyanate prepolymer (Dow) in a 4:1 weight ratio. The mixture was slowly and thoroughly mixed before pouring into a Teflon-coated mold, followed by a two-step curing procedure: (i) ambient conditions for 24 h

acroolecular
Materials and Engineering

www.mame-journal.de

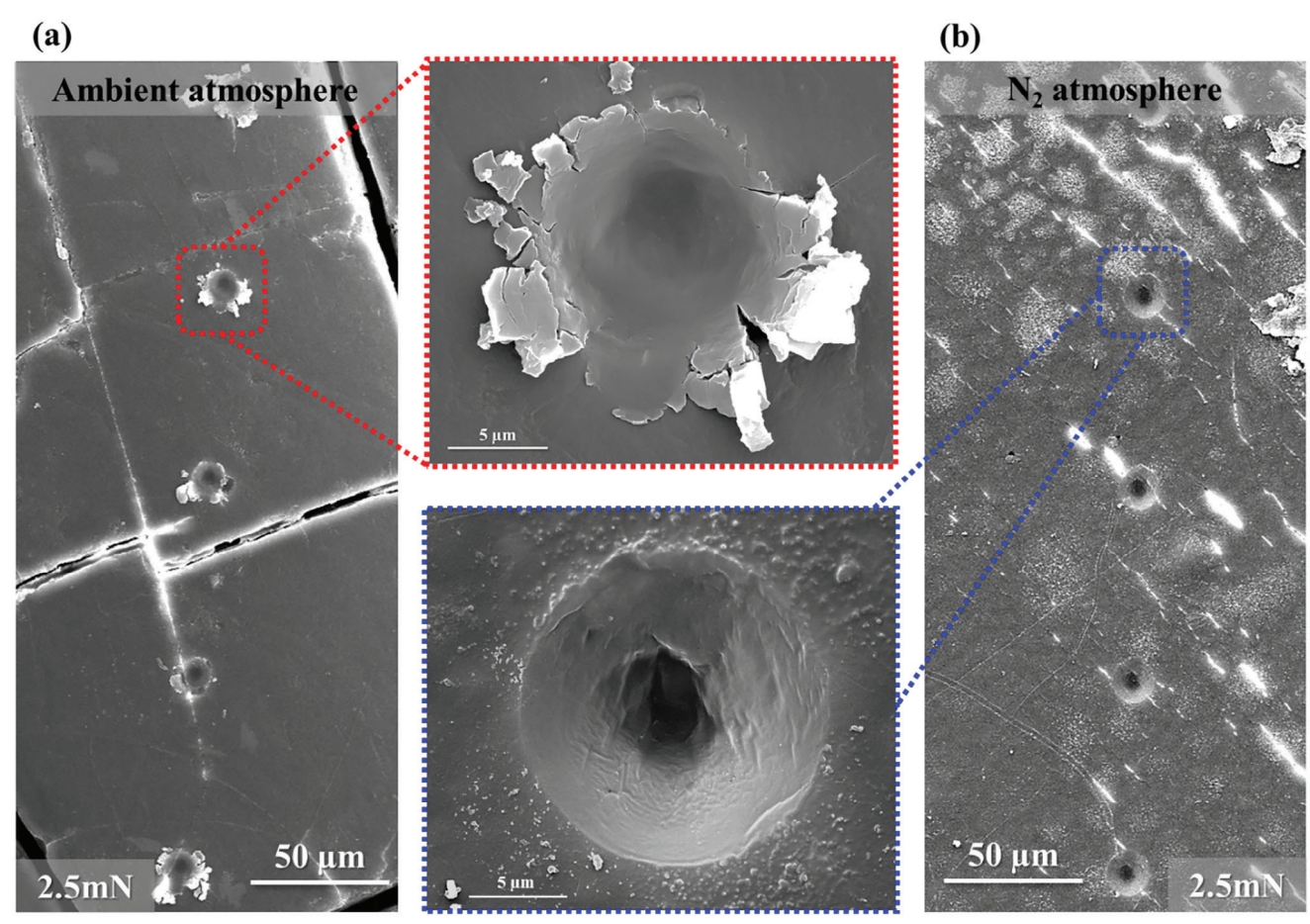


Figure 4. A collage of SEM micrographs differentiating the morphology of nano-impacted polyurea samples after 15 week continuous exposure in a) ambient and b) nitrogen atmospheres with 2.5 mN impact force and 20 μm standoff distance.

and (ii) subsequently vacuum-heated oven at 80 °C for an additional 24 h. Discs ($\phi \approx 25$ mm and thickness of 0.55 \pm 0.05 mm) were extracted and characterized upon curing using a novel nano-impact experiment utilizing a uniquely configured nanoindenter Nanotest Vantage (Micromaterials). The nano-impact measurements consisted of accelerating a hemispherical indenter (5 μ m radius) from a standoff distance (2.5 and 20 μ m) while prescribing an impact load (2.5 and 10 mN), pairing the two extremes to reveal the load-response interrelationship. In one nano-impact loading scenario, the indenter was released from a 20 µm standoff distance from the sample surface with a 2.5 mN load (≈50 nJ). In another nano-impact setting, the conditions included the release from 2.5 µm away from the surface with 10mN indentation force (≈25 nJ) to separate the strain rate effect (by adjusting the standing distance) and load on the nanomechanical response of polyurea. Five distinct locations were subjected to 100 nano-impact repetitions. Indention damage and imprints were analyzed using a scanning electron microscope (SEM), revealing nondetectable cumulative damage after repeated loadings.

Hence, ten additional sample sets extracted from the same sheet were radiated in an ultraviolet enclosure for up to 15 weeks, corresponding to 0.82 years of natural weathering separately under ambient and nitrogen atmospheres. The exposure system consisted of a chamber lined up with mirror-finish stainless steel plates and fitted with four UV bulbs (2 \times Philips TLK40W/03 bulbs with 300 < λ < 460 nm and $\lambda_{\rm peak}\approx$ 360 nm, and 2 \times Philips TLK40W/05 bulbs with 380 < λ < 480 nm and $\lambda_{\rm peak}\approx$ 420 nm). The UV exposure system emitted 5122 mJ cm $^{-2}$ per hour and 8553 mJ cm $^{-2}$ per hour of UV-A and UV-B radiation, respectively, measured using a

radiometer (EIT instrument Powerpuck II).^[8] The first set of samples was withdrawn from the ultraviolet chamber at the end of 3 weeks, followed by the next sets, which were sequentially taken out at equal intervals of 3 weeks until the final set was removed after 15 weeks. A similar procedure was also employed to prepare the polyurea samples exposed to ultraviolet radiation in a nitrogen-rich atmosphere, continuously purged with nitrogen from an N_2 generator (Parker Domnick Hunter). Complementary to this investigation are previous reports culminating in the ultraviolet effects on the properties of thermoset polyurea.^[8,9,12,30–32]

The objective was radiation-induced embrittlement to exaggerate the cumulative damage and delineate the effects of the microsegmented structure of polyurea, as reported a priori. The utilization of different atmospheric conditions was to intentionally induce surface embrittlement as a function of photooxidation and photodegradation processes, respectively, where the ambient atmosphere was previously associated with pronounced structural and mechanical damage. [8,9,12,30,31] The nitrogen curbed the embrittlement effects. [12] The progressive embrittlement damage was demonstrated by removing separate sets within 3-week increments up to the terminal period. After 100 nano-impact repetitions, the impact sites were examined under the SEM (FEI, Quanta 450).

Acknowledgements

The authors acknowledge funding from the United States Department of Defense (N00014-22-1-2376, W911NF1410039, and W911NF1810477) and the National Science Foundation (CMMI-1925539 and DBI-0959908).





www.mame-journal.de

Conflict of Interest

The authors declare no conflict of interest.

Data availability Statement

The data that support the findings of this study are available from the corresponding author upon reasonable request.

Keywords

elastomers, environment-embrittlement, hardening, nano-impact, softening

Received: April 2, 2024 Revised: June 13, 2024 Published online: July 5, 2024

- R. G. S. Barsoum, Elastomeric Polymers with High Rate Sensitivity: Applications in Blast, Shockwave, and Penetration Mechanics, William Andrew, Norwich, NY, USA 2015.
- [2] H. Kim, J. Citron, G. Youssef, A. Navarro, V. Gupta, Mech. Mater. 2012, 45, 10
- [3] I. N. Mforsoh, J. LeBlanc, A. Shukla, Polym. Test. 2020, 85, 106450.
- [4] I. Whitten, G. Youssef, Polym. Degrad. Stab. 2016, 123, 88.
- [5] N. U. Huynh, A. Kumar, M. Ghorbani, G. Youssef, *Polym. Test.* 2023, 129, 108279
- [6] N. U. Huynh, G. Youssef, J. Mech. Phys. Solids 2023, 175, 105297.
- [7] A. Sánchez-Ferrer, D. Rogez, P. Martinoty, Macromol. Chem. Phys. 2010, 211, 1712.
- [8] A. Blourchian, A. M. Shaik, N. U. Huynh, G. Youssef, J. Polym. Res. 2021, 28, 1.
- [9] A. M. Shaik, N. U. Huynh, G. Youssef, Mech. Mater. 2020, 140, 103244.
- [10] T. Zheng, Y. Zhang, J. Shi, J. Xu, B. Guo, Mol. Simul. 2021, 47, 1258.
- [11] T. Li, Z. Xie, J. Xu, Y. Weng, B.-H. Guo, Eur. Polym. J. 2018, 107, 249.

- [12] A. Kumar, D. Pullman, G. Youssef, Spectrochim. Acta, Part A 2024, 309, 123804.
- [13] A. M. Castagna, A. Pangon, T. Choi, G. P. Dillon, J. Runt, Macromolecules 2012, 45, 8438.
- [14] Y. Sun, S. E. Kooi, K. A. Nelson, A. J. Hsieh, D. Veysset, Appl. Phys. Lett. 2020, 117, 021905.
- [15] T. Li, T. Zheng, J. Han, Z. Liu, Z.-X. Guo, Z. Zhuang, J. Xu, B.-H. Guo, Polymers 2019, 11, 838.
- [16] B. Koohbor, N. Pagliocca, G. Youssef, Mech. Mater. 2021, 161, 104006.
- [17] G. Youssef, B. Koohbor, Preparation, Characterization, and Applications of Polyurea Foams (Eds: P. Pasbakhsh, D. Mohotti, K. Palaniandy, S. Auckloo), Elsevier, Amsterdam, Netherlands 2023, pp. 303–321.
- [18] M. Ikeda, M. Aniya, J. Non-Cryst. Solids 2013, 371, 53.
- [19] R. G. Rinaldi, M. C. Boyce, S. J. Weigand, D. J. Londono, M. W. Guise, J. Polym. Sci., Part B: Polym. Phys. 2011, 49, 1660.
- [20] S. I. Rosenbloom, S. J. Yang, N. J. Tsakeredes, B. P. Fors, M. N. Silberstein, *Polymer* 2021, 227, 123845.
- [21] N. U. Huynh, B. Koohbor, G. Youssef, Macromol. Rapid Commun. 2023, 44, 2200725.
- [22] N. U. Huynh, C. Gamez, G. Youssef, Macromol. Mater. Eng. 2022, 307, 2100506.
- [23] T. C. Ransom, M. Ahart, R. J. Hemley, C. M. Roland, *Macromolecules* 2017, 50, 8274.
- [24] C. Roland, J. N. Twigg, Y. Vu, P. H. Mott, Polymer 2007, 48, 574.
- [25] H. Jin, T. Jiao, R. J. Clifton, K.-S. Kim, J. Mech. Phys. Solids 2022, 164, 104898.
- [26] R. P. White, J. E. Lipson, Rubber Chem. Technol. **2019**, 92, 612.
- [27] C. Gong, Y. Chen, T. Li, Z. Liu, Z. Zhuang, B. Guo, H. Wang, L. Dai, Mech. Mater. 2021, 152, 103650.
- [28] W. Nantasetphong, A. V. Amirkhizi, S. Nemat-Nasser, Polymer 2016, 99, 771.
- [29] N. U. Huynh, B. Koohbor, G. Youssef, Mech. Time-Depend. Mater. 2023. 27, 727.
- [30] G. Youssef, J. Brinson, I. Whitten, J. Polym. Environ. 2018, 26, 183.
- [31] G. Youssef, I. Whitten, Mech Time Depend Mater 2017, 21, 351.
- [32] P. Pasbakhsh, K. Palaniandy, S. Auckloo, D. Mohotti, Polyurea Synthesis, Properties, Composites, Production, and Applications, (Eds: P. Pasbakhsh, K. Palaniandy, S. Auckloo, D. Mohotti), Elsevier, Netherlands 2023, pp. 383–391.